CHEMISTRY
AN ASIAN JOURNAL

DOI: 10.1002/asia.201200507

Opp-Dibenzoporphyrins as a Light-Harvester for Dye-Sensitized Solar Cells

Rohit Deshpande,[a] Bo Wang,[a] Lin Dai,[a] Lin Jiang,[a] C. Scott Hartley,[a] Shouzhong Zou,[a] Hong Wang,*[a] and Lei Kerr*[b]

Abstract: New *opp*-dibenzoporphyrins were prepared in a concise method that was based on a Pd^0-catalyzed cascade reaction. These porphyrins, which contained carboxylic-acid linker groups on benzene rings that were fused to the porphyrin at their β,β′-positions, were examined as sensitizers for dye-sensitized solar cells for the first time. Whereas all of the porphyrins showed solar-energy-to-electricity conversion, an *opp*-dibenzoporphyrin with conjugated carboxylic-acid linkers displayed the highest conversion efficiency and an exceptionally high J_{sc} value. Cyclic voltammetry of these porphyrins suggested that the fusion of two aromatic benzene rings onto the periphery of the porphyrin lowered the HOMO–LUMO energy gap; the incorporation of a conjugated carboxylic-acid linker group decreased the HOMO–LUMO gap even further. These CV data are consistent with DFT calculations for these porphyrins and agree well with the UV/Vis absorption- and fluorescence spectra of these porphyrins.

Keywords: benzoporphyrins · cyclic voltammetry · density functional calculations · dyes/pigments · dye-sensitized solar cells

Introduction

Dye-sensitized solar cells (DSSCs) have emerged as a promising photovoltaic technology because they offer the possibility of efficient and inexpensive solar-energy-to-electricity conversion.[1] In recent years, extensive efforts have been devoted to improving the photovoltaic performance and stability of DSSCs. Porphyrins are attractive candidates as light harvesters for DSSCs because of their primary light-harvesting role in nature. Consequently, they have been investigated for applications in DSSCs over the last twenty years.[1a,d,2] However, until recently, the overall performance of porphyrins has been significantly inferior to that of ruthenium–polypyridyl dyes. Early work focused on porphyrins with the linker group (a functional group that is used to connect the dye to the semiconductor electrode, usually a carboxylic acid) attached at the *meso* aryl ring and the resulting DSSCs generally exhibited low solar-energy-to-electricity conversion efficiencies ($<4\%$).[2c,3] Recently, through attachment of the linker group through a conjugated spacer moiety at the β-position of the porphyrin, the solar-energy-to-electricity conversion efficiency (η) was significantly increased.[4] An efficiency of 7.1 % was reported by the Officer and Grätzel groups in 2007. Very recently, a new class of porphyrins has been introduced that contained donor–acceptor features at the *meso*-positions of the porphyrin through a π-conjugated bridge.[5] By co-sensitizing with a metal-free dye that had a complementary spectroscopic response, an unprecedented high efficiency of 11 % was achieved in 2010. By replacing the *tert*-butyl groups with octyloxy groups, a record high efficiency ($\eta = 12.3\%$) was obtained,[5k] the highest efficiency so far for DSSCs.

Although a number of porphyrins have been investigated in DSSCs, only a handful of β-functionalized porphyrins have been reported owing to their synthetic complexity.[6] Porphyrins that are fused with aromatic rings at their β-positions (π-extended porphyrins) are even more rare owing to the limited number of available synthetic approaches; in particular, the marked lack of methods for the functionalization of their periphery severely limits their applications.[7] Only examples of quinoxaline-fused porphyrins are known in the literature, thus leading to a maximum efficiency of 6.3 %.[8] Nevertheless, extended porphyrins appear to be ideal candidates to further explore porphyrins as light-harvesters for solar-energy conversion. Because of the extension of their π-conjugation, the Soret band of those molecules is bathochromically shifted up to 450–550 nm[9] and an enhancement of their Q bands is often observed[9a,4e–h] These features make this class of porphyrin molecules extremely attractive as dye-sensitizers for DSSCs.

Despite recent progress,[9a,b,10] most of the syntheses of π-extended porphyrins that have been reported require harsh conditions and/or lengthy procedures. In particular, the lack

---

[a] R. Deshpande, B. Wang, L. Dai, L. Jiang, Prof. C. S. Hartley,
Prof. S. Zou, Prof. H. Wang
Department of Chemistry and Biochemistry
Miami University, 701 East High Street
Oxford, OH 45056 (USA)
Fax: (+1) 513-529-5715
E-mail: wangh3@muohio.edu

[b] Prof. L. Kerr
Department of Paper and Chemical Engineering
Miami University, 701 East High Street
Oxford, OH 45056 (USA)
Fax: (+1) 513-529-0768
E-mail: kerrll@muohio.edu

of functional groups in these methods makes the design and synthesis of functionalized extended porphyrins challenging. For example, to be used in DSSCs, a carboxylic acid group (that serves to anchor the dye onto the semiconductor (TiO_2) surface) must be attached onto the porphyrins. Very recently, we developed a concise method to prepare functionalized benzoporphyrins.[11] In this method, an alkene reacts with a β,β′-dibromoporphyrin through a three-step cascade reaction that involves a vicinal two-fold Heck reaction, 6π-electrocyclization, and subsequent aromatization. The wide variety of commercially available alkenes and the easy access to bromoporphyrins make it possible to access a relatively large number of functionalized benzoporphyrins. Herein, we report the synthesis and characterization of a series of new *opp*-dibenzoporphyrins and their evaluation as light harvesters in DSSCs.

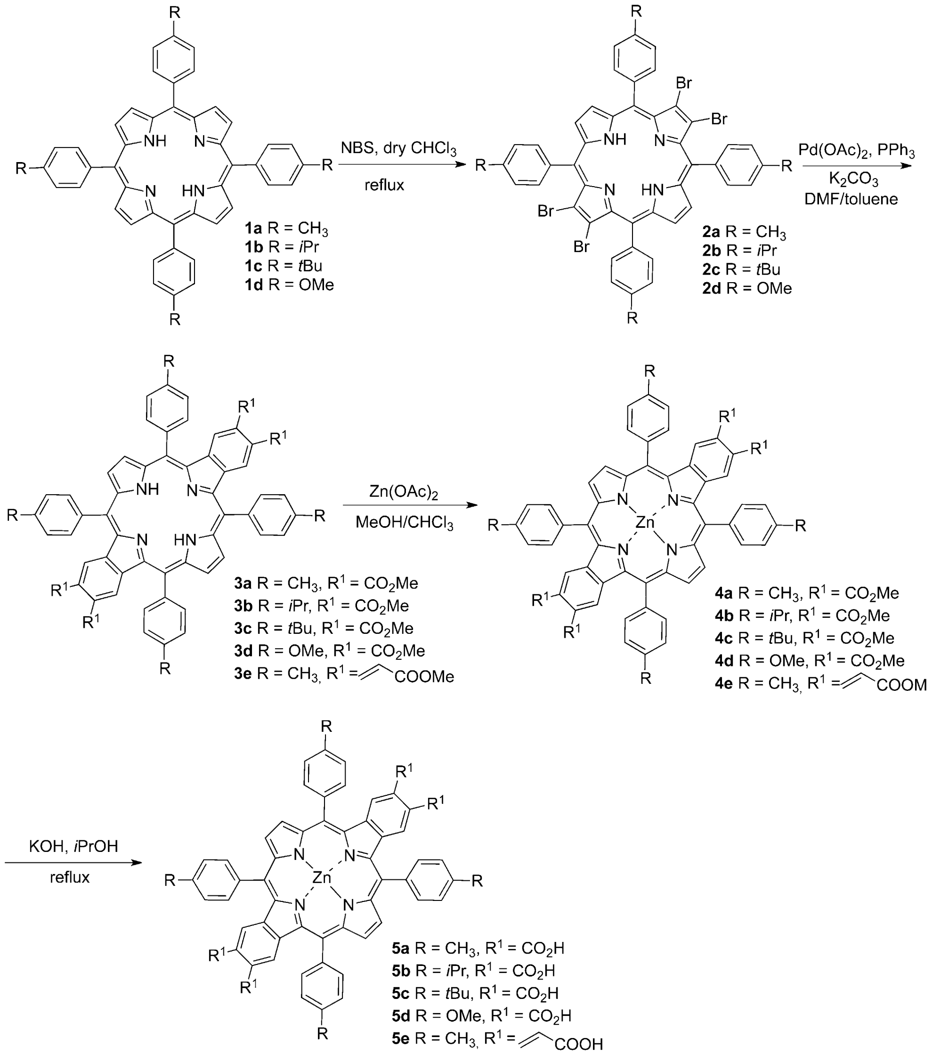

Scheme 1. Synthesis of *opp*-dibenzoporphyrins.

Results and Discussion

Synthesis

The synthesis of *opp*-dibenzoporphyrin dyes is illustrated in Scheme 1. It is widely accepted that porphyrin-aggregation affects solar-cell efficiency. Thus, porphyrins were prepared with increasingly bulky substituents, such as *para*-methyl, *para*-isopropyl, and *para*-*tert*-butyl, on their *meso*-phenyl rings. Tetrabromoporphyrins **2a**–**2d** were readily obtained in high yield (85–95%) through the treatment of corresponding free-base porphyrin **1** with *N*-bromosuccinimide (NBS) in refluxing $CHCl_3$. Tetrabromoporphyrins **2a**–**2d** reacted with methyl acrylate or (*E*)-ethyl-penta-2,4-dienoate through the a Pd^0-catalyzed cascade reaction to afford *opp*-dibenzoporphyrins **3a**–**3e** in 45–60% yield. Metal insertion with $Zn(OAc)_2$ converted free-base porphyrins **3a**–**3e** into Zn^{II}–porphyrins **4a**–**4e** in high yields (85–95%). Hydrolysis of compounds **4a**–**4e** with KOH in refluxing *i*PrOH afforded Zn^{II}–*opp*-dibenzoporphyrins **5a**–**5e** in 65–78% yields, which were suitable for applications in DSSC. The structures of all of these new compounds were verified by ^1H NMR, ^{13}C NMR, and UV/Vis spectroscopy, and by MS (MALDI-TOF).

Optical and Electrochemical Properties

Figure 1 shows the UV/Vis absorption spectra of compounds **5a**–**5e**. Upon fusion of two benzene rings onto the porphyrin framework, the Soret band of compounds **5a**–**5d** was centered at 458 nm, which was about 20–30 nm red-shifted relative to that of their respective parent porphyrins (**1**). The Soret band of compound **5e** was further red-shifted by

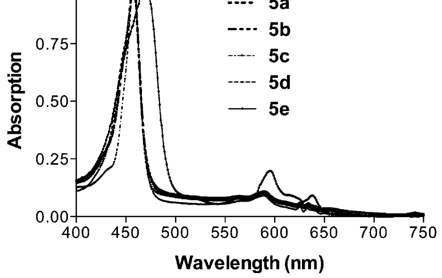

Figure 1. UV/Vis absorption spectra of compounds **5a**–**5e** in MeOH.

11 nm relative to that of compound **5a**–**5d**, owing to the incorporation of conjugated carboxylic-acid linkers onto the porphyrin. The Q bands of compound **5e** were also red-shifted and broadened. The absorption of compound **5e** is expected to have better overlap with the solar spectrum and should be more beneficial for harnessing solar energy.

The steady-state fluorescence spectra of compounds **5a**–**5e** were measured in MeOH by exciting at the position of the strongest Soret absorption (Figure 2). Two emission bands were observed (centered at 638 nm and 703 nm) for compounds **5a**–**5d**. Corresponding to the red-shifting and broadening of the absorption bands, the two emission bands of compound **5e** were also broadened and red-shifted to 643 nm and 708 nm, respectively.

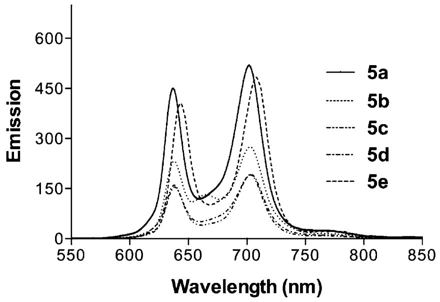

Figure 2. Steady-state fluorescence spectra of compounds **5a**–**5e** in MeOH.

DFT Calculations

To gain insight into the optical- and electrochemical properties of the DSSC-suitable porphyrins (**5a**–**5e**), DFT calculations were performed. From the optimized geometries (Figure 3), all of the porphyrins (**5a**–**5e**) were found to adopt slightly saddled conformations. The electronic absorption of the porphyrins, including both Soret bands and Q bands, is due to π–π* transitions. The frontier orbitals that are responsible for the transitions in the parent porphyrin are two π orbitals (a_{1u} and a_{2u}) and two degenerate π* orbitals (eg_x and eg_y) in the Gouterman four-orbital model.[12] Analogous MOs are predicted for these less-symmetrical (effectively C_{2v}) structures (Figure 4). The calculated energy levels (Table 1) suggest that the LUMO and LUMO+1 remain very nearly degenerate for all of the porphyrins (**5a**–**5e**), owing to the symmetric structure of these porphyrins. The energy levels of the frontier orbitals of compounds **5a**, **5b**, and **5c** are almost identical, which can be explained by the presence of similar alkyl substituents (methyl, *i*Pr, and *t*Bu, respectively) at the *para* positions of the *meso*-phenyl groups. When the substituents at the *para* position of the *meso*-phenyl ring are replaced by methoxy groups (**5d**), both the HOMO and the LUMO energy levels move up slightly (by about 0.06 eV relative to those of compound **5a**), whilst the HOMO–LUMO energy gap (about 2.67 eV) remains unchanged. The LUMO and LUMO+1 of compound **5e** are essentially degenerate, but the HOMO−1 and HOMO are further apart than those of compounds **5a**–**5c**. Comparison of compound **5e** with compound **5a** suggests that the incorporation of conjugated carboxylic-acid linkers leads to a smaller HOMO–LUMO energy gap (by 0.13 eV), which can be ascribed to a much-lower-energy LUMO because the HOMO is almost unchanged. These effects are

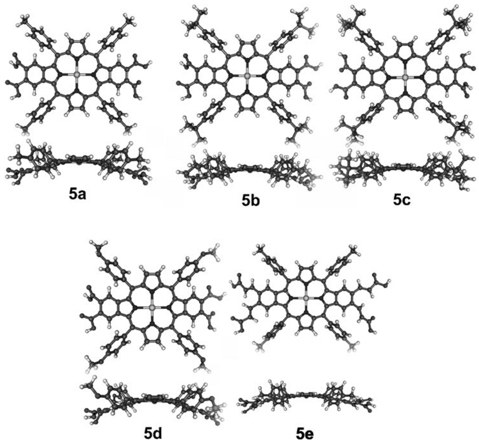

Figure 3. Molecular geometries of compounds **5a**–**5e**, calculated at the B3LYP/6-31G(d) level of theory.

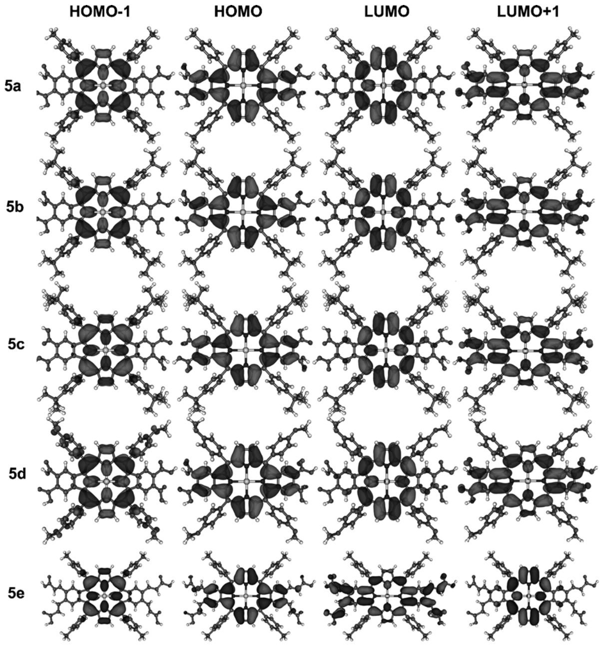

Figure 4. Molecular orbitals of compounds **5a**–**5e**, calculated at the B3LYP/6-31G(d) level of theory.

Table 1. Calculated molecular-orbital energy levels in compounds **5a**–**5e**.

Compound	HOMO−1	HOMO	LUMO	LUMO+1
5a	−5.25	−5.13	−2.46	−2.43
5b	−5.27	−5.14	−2.47	−2.44
5c	−5.26	−5.13	−2.46	−2.43
5d	−5.12	−5.07	−2.40	−2.38
5e	−5.34	−5.11	−2.57	−2.53

consistent with the observed red-shifting- and broadening in the absorption and emission spectra of compound **5e** upon the introduction of conjugated linker groups onto the fused benzene rings of the porphyrin. The HOMOs of compounds **5a**–**5e** involve heavy participation of the fused benzene rings. Whereas the LUMO of compounds **5a**–**5d** mainly remains on the porphyrin core, the LUMO of compound **5e** engages both the fused benzene rings and the conjugated linker groups.

Cyclic voltammetry (CV) was used to determine the redox potentials of these porphyrins (Figure 5). The first oxidation potentials of both dibenzoporphyrins **5a** and **5b** were negatively shifted by 100 mV compared with their respective parent porphyrins, thus indicating an increase in the HOMO energy level by 0.1 eV upon fusion of two benzene rings on the porphyrin periphery. The LUMO energy level remained almost unchanged (only decreased by about 0.03 eV; Figure 5a,b). The smaller HOMO–LUMO energy gap corresponded to their red-shifted electronic absorption. Owing to the low solubility of compounds **5d** and **5e** in *N*,*N*-dimethylformamide (DMF), the CVs of compounds **4d** and **4e** were measured instead, assuming that there was no significant difference between the electronic properties of the carboxylic-acid group and the methyl-ester group. For comparison, the CV of compound **4a** was also measured; the potentials are collected in Table 2. The peak potential for the first reduction (about −1.0 V) was almost unchanged for compounds **4a**, **4d**, and **4e**. However, the difference comes on the addition of a second electron: Compound **4e** is more readily reduced than compounds **4a** and **4d**. For the first oxidation (the peak is at around +1.0 V), compound **4e** is about 50 mV more easily oxidized than both compounds **4a** and **4d**. These data suggest that compound **4e** has the smallest HOMO–LUMO energy gap, whilst compounds **4a** and **4d** have similar HOMO–LUMO energy gaps. The incorporation of conjugated linker groups decreases the HOMO–LUMO energy gap, which is consistent with the red shifts in both the Soret- and Q bands in the electronic absorption spectra. These data also agree well with the DFT calculations.

Table 2. Oxidation/reduction potentials [V] of porphyrins **4a**, **4d**, and **4e**.

Compound	*V* (versus SCE)		
	−1 to −2	0 to −1	0 to +1
4a	−1.40	−1.00	+1.06
4d	−1.40	−1.00	+1.04
4e	−1.30	−1.00	+1.01

Photovoltaic Properties of Porphyrin-Sensitized TiO_2 Solar Cells

The amount of dye that is adsorbed onto a TiO_2 surface influences the efficiency of the cell. To obtain an optimized solar-energy-to-electricity conversion, a concentration study was performed with compound **5b**. The TiO_2 electrode was immersed in solutions of the porphyrin (**2b**) in EtOH for 12 h. The efficiency (η) of solar-energy-to-electricity conversion was calculated according to $\eta = J_{sc} \times V_{oc} \times FF$ (J_{sc} = short-circuit current density, V_{oc} = open-circuit voltage, FF = fill factor). As listed in Table 3, the highest efficiency of solar-energy-to-electricity conversion was obtained at 0.2 mM. At lower concentration, the conversion efficiency was also lower, which may be due to the insufficient adsorption of the dye; when higher concentrations were used, a decreasing trend of conversion efficiency was clearly observed. This decreasing efficiency was likely due to more serious aggregation of the porphyrin at higher concentrations. On the other hand, the excess dye molecules blocked the subsequent layers of the dye next to the TiO_2 surface from being exposed to the redox species and impeded the dye regeneration,

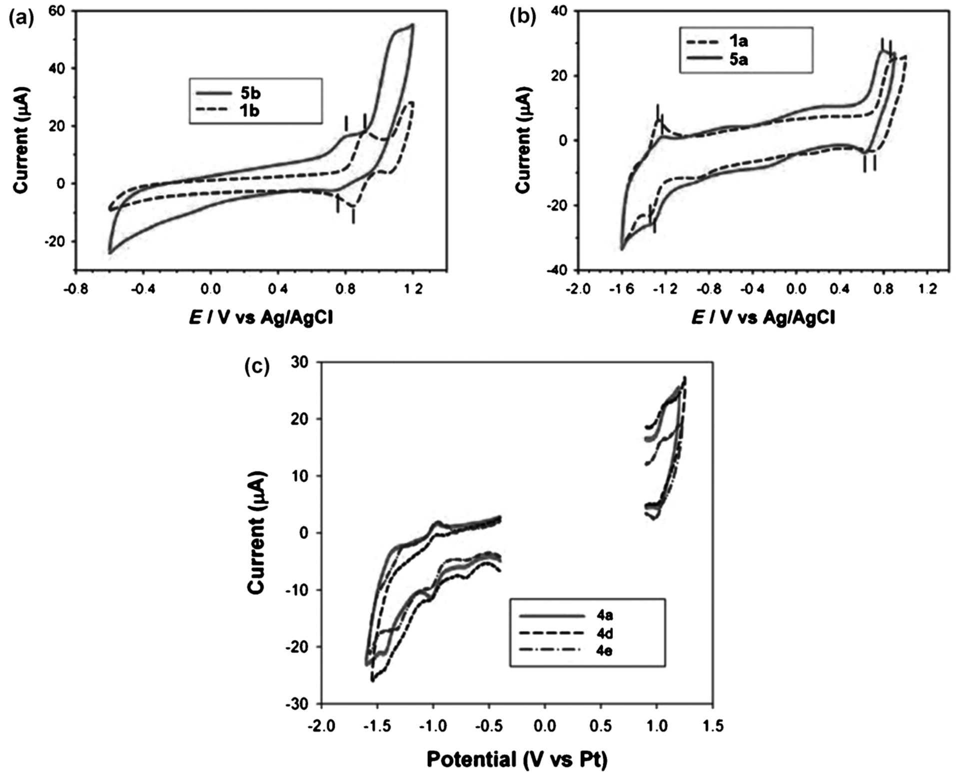

Figure 5. Cyclic voltammograms of porphyrins in DMF that contained 0.1 M TBAP; scan rate: 0.1 V s^{-1}. a) **1b** and **5b**; b) **1a** and **5a**; c) **4a**, **4d**, and **4e**.

Table 3. Concentration study of porphyrin **5b**.

Concentration [mM]	J_{sc} [mA cm^{-2}]	V_{oc} [V]	*FF*	Efficiency [%]
0.1	3.61	0.5	0.45	0.82
0.2	6.26	0.54	0.47	1.59
0.3	4.27	0.54	0.46	1.06
0.4	3.41	0.53	−0.46	0.82
0.5	1.28	1.05	0.41	0.54

thereby resulting in a lower efficiency of solar-energy-to-electricity conversion in the DSSCs.

Table 4. Photovoltaic performance of DSSCs that were based on *opp*-dibenzoporphyrins **5a**–**5e**.

Dye	J_{sc} [mA cm^{-2}]	V_{oc} [V]	*FF*	Efficiency [%]
N719	19.6	0.72	0.57	7.98
5a	8.86	0.57	0.58	2.93
5b	5.05	0.54	0.56	1.54
5c	5.52	0.58	0.57	1.81
5d	7.48	0.57	0.53	2.22
5e	12.87	0.53	0.46	3.14

Then, the optimized concentration (0.2 mm in EtOH) was used for modifying the TiO_2 electrode with other porphyrins (**5a**, **5c**–**5e**); the data for the solar-cell performance of compounds **5a**–**5e** are listed in Table 4. N719 dye ($[RuL_2(NCS)_2]$:2TBA, L = 2,2′-bipyridyl-4,4′-dicarboxylic acid, TBA = tetra-*n*-butylammonium) on TiO_2 was used as a reference material. Compounds **5a**, **5b**, and **5c** were prepared to understand how porphyrin-aggregation affected the efficiency of solar-energy-to-electricity conversion of the DSSC. Compound **5c** contains the most bulky group on the *meso*-phenyl rings of the porphyrin and are expected to have the smallest aggregation effect compared with compounds **5a** and **5b.** It is generally understood that the lower the aggregation effect, the higher the solar-energy conversion. Owing to similar alkyl substitutions on the *meso*-phenyl rings of the porphyrins, the optical- and electrochemical properties of compounds **5a**, **5b**, and **5c** are almost identical. Contrary to this generally accepted view, compound **5a**, which is expected to have the highest aggregation effect, displayed the highest efficiency for solar-energy-to-electricity conversion ($\eta = 2.93\,\%$). The lower efficiency of compound **5c** is attributed to its much lower J_{sc} value. The UV/Vis absorption spectra of the dye solutions before and after immersion of the TiO_2 electrode are shown in Figure 6. Compound **5a** displays a much bigger difference between the absorptions before and after adsorption of the dye relative to that of compound **5c**, thus implying that a larger amount of compound **5a** was adsorbed onto the TiO_2 surface than that of compound **5c** under similar conditions (0.2 mm, 12 h). It is likely that the lower J_{sc} values of compounds **5b** and **5c** resulted from the smaller amounts of porphyrin dyes that were present on the TiO_2 surface and the aggregation effect did not play a role in determining the solar-conversion efficiencies of these porphyrins under the above-mentioned conditions.

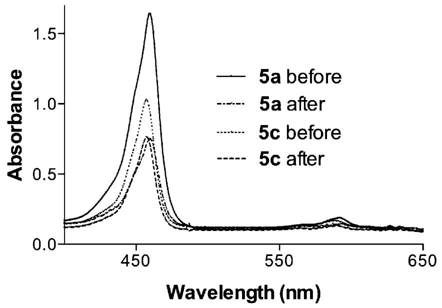

Figure 6. UV/Vis absorption spectra of compounds **5a** and **5c**. Before: before adsorption on the TiO_2 surface; after: after adsorption on the TiO_2 surface.

The efficiency of solar-energy-to-electricity conversion of compound **5d** was 2.22 %, which was smaller than that of compound **5a**. This result can be explained by a slight increase in the HOMO–LUMO gap of compound **5a**, owing to the introduction of strongly electron-donating methoxy groups at the *para* positions of the *meso*-phenyl rings. The highest solar-conversion efficiency was obtained with compound **5e**, which possessed a more extended π system than compounds **5a**–**5d**. The UV/Vis spectra of compound **5e** showed much more broadened and red-shifted absorption bands. This feature is expected to bring broader overlap with the solar spectrum and, thus, enhanced solar-energy conversion. Notably, the J_{sc} value of compound **5e** (12.87) is exceptionally high and comparable to that of the best-performing porphyrin dye in a DSSC.[5a–h] This result suggests that attaching conjugated linkers can considerably change the electronic profile of the porphyrin dye and, thus, significantly enhance the light-harvesting capability of the porphyrin dye.

Conclusions

New *opp*-dibenzoporphyrins have been synthesized through a Pd^0-catalyzed cascade reaction. These *opp*-dibenzoporphyrins were evaluated for the first time as a light harvester for dye-sensitized solar cells. These porphyrins displayed moderate solar-energy-to-electricity conversion efficiencies of 1.54–3.14 %. Our study shows that the installation of a more bulky group on the *meso*-phenyl rings of the porphyrin did not help enhance the solar-energy conversion, presumably owing to lower adsorption of the porphyrin dye on the TiO_2 surface. The incorporation of conjugated carboxylic-acid linkers onto the porphyrin considerably broadened and red-shifted the absorption bands of the porphyrin, thereby leading to a very high J_{sc} value (12.89), which is comparable to the highest reported values of porphyrin dyes for DSSC. The electronic and optical properties of these compounds were measured by using UV/Vis spectroscopy, steady-state fluorescence spectrometry, and cyclic voltammetry, and these data correlated well with DFT calculations.

Experimental Section

General

All solvents were of analytical grade unless otherwise stated and were either obtained from Sigma–Aldrich or from ACROS. TLC was performed on Silicycle UltraPure Silica Gel 60 F254 TLC plates. Preparative column chromatography was performed on silica gel (40–60 μm) that was purchased from Silicycle. ^{1}H NMR and ^{13}C NMR spectroscopy was performed on a Bruker Avance 500 NMR spectrometer. All samples were prepared in either $CDCl_3$ or CD_3OD. The chemical shifts in the ^{1}H NMR spectra were referenced to $CDCl_3$ at $\delta = 7.24$ ppm or to CD_3OD at $\delta = 4.78$ and 3.35 ppm. The chemical shifts in the ^{13}C NMR spectra were referenced to $CDCl_3$ at $\delta = 77$ ppm or to CD_3OD at $\delta = 49.3$ ppm. UV/Vis spectra were recorded on an Agilent 8453 UV/Vis spectrometer in CH_2Cl_2 or MeOH. MS was performed on a Bruker MALDI-TOF mass spectrometer. Melting points were measured on an Electrothermal MEL-TEMP apparatus and were uncorrected.

DFT Calculations

Gaussian 03 (Rev. D.02) calculations were performed on the Redhawk computer cluster at Miami University. Following geometry-optimizations, vibrational-frequency analysis was used to ensure that all of the stationary points were energy minima. Geometry-optimization and electronic-structure calculations of the porphyrins were performed by using the B3LYP functional and the 6–31G(d) basis set. Molecular orbitals were visualized by using Molekel 5.4.0.8.[13]

Electrochemistry

Cyclic voltammograms were recorded with a three-electrode cell and a CHI 750 electrochemical analyzer. A Au coil was used as the working electrode, a Pt coil was used as the counter electrode, and a Pt disk served and the quasi-reference electrode.

Photovoltaic Measurements

The porphyrin molecules were sensitized on TiO_2 to test the solar-cell efficiency. The TiO_2-film method used herein was based on that reported by Nazeeruddin et al. in 1993.[14] Commercial TiO_2 (P25, Degussa AG, Germany), acetylacetone, and Triton X-100 were used to make TiO_2 paste. A doctor-blade method was used to spread the paste onto SnO_2:F (FTO) glass. Samples were then annealed at 450 °C for 30 min.

Synthesis

Compounds **1** were prepared according to literature procedures.[15]

Synthesis of Tetrabromoporphyrins 2

A mixture of porphyrin **1** (0.4 g, 0.5 mmol) and NBS (0.6 g, 3.3 mmol) in dry $CHCl_3$ (120 mL) was heated at reflux in a 250 mL round-bottomed flask overnight. The progress of the reaction was monitored by TLC ($CHCl_3$/cyclohexane, 1:1). The reaction mixture was then cooled to RT and filtered through a short plug of silica gel (CH_2Cl_2). The filtrate was evaporated to dryness and recrystallized from CH_2Cl_2/MeOH to give compound **2**.

2b: Dark-brown powder (93 %); m.p. > 310 °C; ^{1}H NMR (500 MHz, $CDCl_3$, 25 °C, TMS): $\delta = 8.71$ (s, 4H; β-H), 8.08 (d, ^3J(H,H) = 8.0 Hz, 8H; *o*-Ph-H), 7.62 (d, ^3J(H,H) = 8.0 Hz, 8H; *m*-Ph-H), 3.23 (m, 4H; isopropyl CH), 1.51 (d, ^3J(H,H) = 7.0 Hz, 24H; isopropyl CH_3), −2.76 ppm (s, 2H; inner H); ^{13}C NMR (125 MHz, 25 °C, TMS): $\delta = 24.37$, 34.19, 120.41, 124.69, 125.65, 135.68, 138.10, 140.39, 148.42, 149.62 ppm; UV/Vis (CH_2Cl_2): λ_{max} (log ε) = 442 (5.66), 542 (4.89), 692 (4.85), 628 (4.83), 634 nm (4.80); HRMS (MALDI-TOF): *m*/*z* calcd for $C_{56}H_{50}Br_4N_4$: 1098.640; found: 1098.542.

2c: Dark-brown powder (85 %); m.p. > 310 °C; ^{1}H NMR (500 MHz, $CDCl_3$, 25 °C, TMS): $\delta = 8.72$ (s, 4H; β-H), 8.08 (d, ^3J(H,H) = 8.0 Hz, 8H; *o*-Ph-H), 7.65 (d, ^3J(H,H) = 8.0 Hz 4H; *m*-Ph-H), 1.57 (s, 36H; *tert*-butyl-H), −2.76 ppm (s, 2H; inner H); UV/Vis (CH_2Cl_2): λ_{max} (log ε) = 432 (5.66), 533 (4.56), 673 (4.35), 604 (4.19), 625 nm (4.15); these spectroscopic data are in agreement with the literature values.[11]

*Synthesis of Free-Base opp-Dibenzoporphyrins **3 a–3 e***

Tetrabromoporphyrin **2** (0.045 mmol), palladium acetate (5.12 mg, 0.023 mmol), triphenylphosphine (15.54 mg, 0.059 mmol), and K_2CO_3 (26.16 mg, 0.19 mmol) were added to a Schlenk flask and dried under vacuum. The vacuum was released under an argon atmosphere to allow for the addition of DMF (7 mL), dry toluene (9 mL), and methyl acrylate or (*E*)-methyl-penta-2,4-dienoate (1.35 mmol). Then, the mixture was degassed by four freeze–pump–thaw cycles and the flask was purged with argon again. The Schlenk flask was sealed and heated at reflux for 72 h. The solvent was removed and the residue was subjected to preparative column chromatography on silica gel (CH_2Cl_2). The band that contained the desired porphyrin was collected and recrystallized from $CHCl_3$/MeOH.

3a: Reddish-brown crystals (60 %); m.p. > 330 °C; ^{1}H NMR (500 MHz, $CDCl_3$, 25 °C, TMS): $\delta = 8.85$ (s, 4H; β-H), 8.05 (d, ^3J(H,H) = 8.0 Hz, 8H; *o*-Ph-H), 7.65 (d, ^3J(H,H) = 7.5 Hz, 8H; *m*-Ph-H), 7.37 (s, 4H; fused-benzene-H), 3.90 (s, 12H; OCH_3), 2.76 (s, 12H; CH_3), −2.66 ppm (s, 2H; inner H); ^{13}C NMR (125 MHz, 25 °C, TMS): $\delta = 21.62$, 29.71, 52.48, 118.19, 125.76, 127.90, 128.60, 129.06, 138.63, 138.73, 139.16, 142.70, 148.73, 168.43 ppm; IR: $\tilde{\nu} = 3001$, 2962, 2919, 2850, 1712, 1419, 1358, 1259, 1219, 1091, 1009, 901, 791, 701 cm^{-1}; UV/Vis (CH_2Cl_2): λ_{max} (log ε) = 443 (6.02), 534 (5.21), 568 (5.19), 610 (5.16), 628 nm (5.15); MS (MALDI-TOF): *m*/*z* calcd for $C_{64}H_{50}N_4O_8$: 1002.363; found: 1002.253.

3b: Reddish-brown crystals (55 %); m.p. > 320 °C; ^{1}H NMR (500 MHz, $CDCl_3$, 25 °C, TMS): $\delta = 8.82$ (s, 4H; β-H), 8.10 (d, ^3J(H,H) = 7.5 Hz, 8H; *o*-Ph-H), 7.68 (d, ^3J(H,H) = 7.5 Hz, 8H; *m*-Ph-H), 7.39 (s, 4H; fused-benzene-H), 3.85 (s, 12H; OCH_3), 3.30 (m, 4H, isopropyl CH), 1.58 (d, ^3J(H,H) = 7.0 Hz, 24H; isopropyl CH_3), −2.60 ppm (s, 2H; inner H); ^{13}C NMR (125 MHz, $CDCl_3$, 25 °C, TMS): $\delta = 24.43$, 34.35, 52.46, 119.03, 125.35,125.96, 127.93, 129.10, 133.89, 138.95, 139.24, 142.55, 148.72 149.85, 168.57 ppm; IR: $\tilde{\nu} = 2961$, 2919, 2850, 1735, 1459, 1375, 1259, 1089, 864, 691 cm^{-1}; UV/Vis (CH_2Cl_2): λ_{max} (log ε) = 444 (6.43), 534 (5.43), 568 (5.32), 611 nm (5.29); MS (MALDI-TOF): *m*/*z* calcd for $C_{72}H_{66}N_4O_8$: 1114.488; found: 1114.455.

3c: Reddish-brown crystals (48 %); m.p. > 330 °C; ^{1}H NMR (500 MHz, $CDCl_3$, 25 °C, TMS): $\delta = 8.83$ (s, 4H; β-H), 8.11 (d, ^3J(H,H) = 8.0 Hz, 8H; *o*-Ph-H), 7.83 (d, ^3J(H,H) = 8.0 Hz, 8H; *m*-Ph-H), 7.39 (s, 4H; fused-benzene-H), 3.84 (s, 12H; OCH_3), 1.64 (s, 36H; *tert*-butyl-H), −2.57 ppm (s, 2H; inner H); ^{13}C NMR (125 MHz, $CDCl_3$, 25 °C, TMS): $\delta = 31.74$, 35.07, 52.48, 118.97, 124.80, 125.26, 127.93, 129.10, 133.68, 138.53, 139.22, 142.49, 148.53, 152.21, 168.43 ppm; IR: $\tilde{\nu} = 3001$, 2962, 2919, 2850, 1712, 1419, 1358, 1259, 1219, 1091, 1009, 901, 791, 701 cm^{-1}; UV/Vis (CH_2Cl_2): λ_{max} (log ε) = 440 (5.64), 530 (5.21), 566 nm (5.20); MS (MALDI-TOF): *m*/*z* calcd for $C_{76}H_{74}N_4O_8$: 1170.551; found: 1170.455.

3d: Brown solid (52 %); m.p. > 330 °C; ^{1}H NMR (500 MHz, $CDCl_3$, 25 °C, TMS): $\delta = 8.87$ (s, 4H; β-H), 8.06 (d, ^3J(H,H) = 8.0 Hz, 8H; *o*-Ph-H), 7.40 (s, 4H; fused-benzene-H), 7.35 (d, ^3J(H,H) = 8.0 Hz, 8H; *m*-Ph-H), 4.13 (s, 12H; OCH_3), 3.90 (s, 12H; OCH_3), −2.64 ppm (s, 2H; inner H); ^{13}C NMR (125 MHz, $CDCl_3$, 25 °C, TMS): $\delta = 52.48$, 55.74, 113.48, 118.63, 125.74, 127.89, 129.05, 134.03, 134.81, 139.41, 142.61, 149.05, 160.43, 168.43 ppm; IR: $\tilde{\nu} = 3001$, 2962, 2919, 2850, 1712, 1419, 1358, 1259, 1219, 1091, 1009, 901, 791, 701 cm^{-1}; UV/Vis (CH_2Cl_2): λ_{max} (log ε) = 444 (6.02), 534 (5.00), 610 (4.71), 634 nm (4.53); MS (MALDI-TOF): *m*/*z* calcd for $C_{64}H_{50}N_4O_{12}$: 1066.343; found: 1066.293.

3e: Brown solid (45 %); m.p. > 330 °C; ^{1}H NMR (500 MHz, $CDCl_3$, 25 °C, TMS): $\delta = 8.84$ (s, 4H; β-H), 8.13 (d, ^3J(H,H) = 15.5 Hz, 4H; alkenyl protons), 8.05 (d, ^3J(H,H) = 7.5 Hz, 8H; *o*-Ph-H), 7.68 (d, ^3J(H,H) = 7.5 Hz, 8H; *m*-Ph-H), 7.29 (s, 4H; fused-benzene-H), 6.05 (d, ^3J(H,H) = 15.5 Hz, 4H; alkenyl protons), 3.89 (s, 12H; OCH_3), 2.81 (s, 12H; CH_3), −2.61 ppm (s, 2H; inner H); UV/Vis (CH_2Cl_2): λ_{max} (log ε) = 461 (6.08), 488 (5.99), 580 (4.31) 618 (4.16), 675 nm (3.83); MS (MALDI-TOF): *m*/*z* calcd for $C_{72}H_{58}N_4O_8$: 1107.250; found: 1108.002.

*Synthesis of Zn^{II}–opp-Dibenzoporphyrins **4 a–4 e***

A mixture of porphyrin **3** (0.042 mmol) and $Zn(OAc)_2$ (6.0 equiv) in $CHCl_3$/MeOH (18 mL:6 mL) was heated at reflux for 1 h. Upon completion of the reaction (monitored by TLC), the solvent was evaporated and the residue was subjected to column chromatography on silica gel (CH_2Cl_2). The fraction that contained the desired compound was collected and recrystallized from CH_2Cl_2/MeOH.

4a: Greenish-brown solid (90%); m.p. > 330 °C; ^{1}H NMR (500 MHz, $CDCl_3$, 25 °C, TMS): $\delta = 8.85$ (s, 4H; β-H), 7.95 (d, ^3J(H,H) = 7.5 Hz, 8H; *o*-Ph-H), 7.62 (d, ^3J(H,H) = 8.0 Hz, 8H; *m*-Ph-H), 7.41 (s, 4H; fused-benzene-H), 3.72 (s, 12H; OCH_3), 2.76 ppm (s, 12H; CH_3); ^{13}C NMR (125 MHz, $CDCl_3$, 25 °C, TMS): $\delta = 22.60$, 53.46, 119.98, 126.75, 128.90, 129.73, 130.05, 134.58, 139.62, 139.72, 140.15, 143.63, 149.71, 169.42 ppm; IR: $\tilde{\nu} = 3001$, 2956, 2921, 2850, 1710, 1427, 1336, 1253, 998, 791, 764, 670 cm^{-1}; UV/Vis (CH_2Cl_2): λ_{max} (log ε) = 450 (5.88), 581 (5.30), 627 nm (5.26); MS (MALDI-TOF): *m/z* calcd for $C_{64}H_{48}N_4O_8Zn$: 1064.402; found: 1064.139.

4b: Greenish-brown solid (93%); m.p. > 330 °C; ^{1}H NMR (500 MHz, $CDCl_3$, 25 °C, TMS): $\delta = 8.81$ (s, 4H; β-H), 8.02 (d, ^3J(H,H) = 7.5 Hz, 8H; *o*-Ph-H), 7.63 (d, ^3J(H,H) = 8.0 Hz, 8H; *m*-Ph-H), 7.36 (s, 4H; fused-benzene-H), 3.59 (s, 12H; OCH_3), 3.28 (m, 4H; isopropyl CH), 1.56 ppm (d, ^3J(H,H) = 7.0 Hz, 24H; isopropyl CH_3); ^{13}C NMR (125 MHz, $CDCl_3$, 25 °C, TMS): $\delta = 24.44$, 34.29, 52.28, 119.74, 125.60, 127.99, 131.56, 133.35, 139.96, 140.37, 143.89, 149.32, 150.62, 168.32 ppm; IR: $\tilde{\nu} = 3001$, 2956, 2919, 2850, 1719, 1429, 1350, 1250, 1105, 1018, 972, 837, 791, 764, 693 cm^{-1}; UV/Vis (CH_2Cl_2): λ_{max} (log ε) = 451 (6.25), 582 (5.36), 622 nm (5.22); MS (MALDI-TOF): *m/z* calcd for $C_{72}H_{64}N_4O_8Zn$: 1176.402; found: 1176.366.

4c: Greenish-brown solid (95%); m.p. > 330 °C; ^{1}H NMR (500 MHz, $CDCl_3$, 25 °C, TMS): $\delta = 8.80$ (s, 4H; β-H), 8.02 (d, ^3J(H,H) = 7.5 Hz, 8H; *o*-Ph-H), 7.76 (d, ^3J(H,H) = 8.0 Hz, 8H; *m*-Ph-H), 7.26 (s, 4H; fused-benzene-H), 3.49 (s, 12H; OCH_3), 1.60 ppm (s, 36H; *tert*-butyl-H); ^{13}C NMR (125 MHz, $CDCl_3$, 25 °C, TMS): $\delta = 31.77$, 34.99, 52.28, 119.58, 124.38, 125.39, 127.71, 131.54, 133.18, 139.61, 140.30, 143.75, 150.63, 151.57, 168.26 ppm; IR: $\tilde{\nu} = 3001$, 2962, 2919, 2850, 1712, 1419, 1358, 1259, 1219, 1091, 1009, 901, 791, 701 cm^{-1}; UV/Vis (CH_2Cl_2): λ_{max} (log ε) = 451 (6.02), 581 (4.71), 556 nm (4.60); MS (MALDI-TOF): *m/z* calcd for $C_{76}H_{72}N_4O_8Zn$: 1232.464; found: 1232.479.

4d: Greenish solid (85%); m.p. > 330 °C; ^{1}H NMR (500 MHz, $CDCl_3$, 25 °C, TMS): $\delta = 8.83$ (s, 4H; β-H), 7.96 (d, ^3J(H,H) = 6.5 Hz, 8H; *o*-Ph-H), 7.45 (s, 4H; fused-benzene-H), 7.29 (d, ^3J(H,H) = 6.5 Hz, 8H; *m*-Ph-H), 4.09 (s, 12H; OCH_3), 3.77 ppm (s, 12H; OCH_3); ^{13}C NMR (125 MHz, $CDCl_3$, 25 °C, TMS): $\delta = 52.91$, 56.24, 113.98, 119.14, 126.24, 128.40, 129.55, 134.54, 135.32, 139.92, 143.11, 149.55, 160.94, 168.88 ppm; IR: $\tilde{\nu} = 3001$, 2962, 2919, 2850, 1712, 1419, 1358, 1259, 1219, 1091, 1009, 901, 791, 701 cm^{-1}; UV/Vis (CH_2Cl_2): λ_{max} (log ε) = 452 (6.20), 580 (5.50), 625 nm (5.42); MS (MALDI-TOF): *m/z* calcd for $C_{64}H_{48}N_4O_{12}Zn$: 1128.256; found: 1128.075.

4e: Greenish-brown solid (84%); m.p. > 330 °C; ^{1}H NMR (500 MHz, $CDCl_3$, 25 °C, TMS): $\delta = 8.85$ (s, 4H; β-H), 7.97 (d, ^3J(H,H) = 7.5 Hz, 8H; *o*-Ph-H), 7.82 (d, ^3J(H,H) = 15.5 Hz, 8H; alkenyl protons), 7.63 (d, ^3J(H,H) = 7.5 Hz, 8H; *m*-Ph-H) 7.29 (s, 4H; fused-benzene-H), 5.91 (d, ^3J(H,H) = 15.5 Hz, 4H; alkenyl protons), 3.76 (s, 12H; OCH_3), 2.78 ppm (s, 12H; CH_3); UV/Vis (CH_2Cl_2): λ_{max} (log ε) = 471 (6.03), 596 (4.51), 631 (5.25) 636 nm (4.24); MS (MALDI-TOF): *m/z* calcd for $C_{72}H_{56}N_4O_8Zn$: 1170.620; found: 1170.230.

Synthesis of Porphyrins 5a–5e

A mixture of porphyrin **4** (0.033 mmol) and KOH (1.05 mmol) in isopropanol/H_2O (15 mL:7 mL) was under reflux overnight. Upon completion of the reaction (monitored by TLC), the solvent was removed and the residue was purified by column chromatography on silica gel. The column was first eluted with CH_2Cl_2/MeOH (50:1) to separate the incompletely hydrolyzed products and then with MeOH to collect the desired product. The solvent was removed under reduced pressure and the residue was recrystallized from MeOH/CH_2Cl_2.

5a: Greenish-brown solid (78%); m.p. > 330 °C; ^{1}H NMR (500 MHz, $CDCl_3$, 25 °C, TMS): $\delta = 8.65$ (s, 4H; β-H), 7.95 (d, ^3J(H,H) = 7.0 Hz, 8H; *o*-Ph-H), 7.58 (d, ^3J(H,H) = 7.0 Hz, 8H; *m*-Ph-H), 8.16 (s, 4H; fused-benzene-H), 2.70 ppm (s, 12H; CH_3); IR: $\tilde{\nu} = 3300$–2800(broad), 3127, 3040, 2809, 1706, 1540, 1440, 1401, 1337, 1284, 1121, 992, 793, 759, 693 cm^{-1}; UV/Vis (CH_2Cl_2): λ_{max} (log ε) = 457 (5.71), 589 (4.91), 627 nm (4.80); MS (MALDI-TOF): *m/z* calcd for $C_{60}H_{40}N_4O_8Zn$: 1010.392; found: 1011.0.

5b: Greenish-brown solid (78%); m.p. > 330 °C; ^{1}H NMR (500 MHz, $CDCl_3$, 25 °C, TMS): $\delta = 8.60$ (s, 4H; β-H), 7.92 (d, ^3J(H,H) = 7.5 Hz, 8H; *o*-Ph-H), 7.54 (d, ^3J(H,H) = 7.5 Hz, 8H; *m*-Ph-H), 7.96 (s, 4H; fused-benzene-H), 3.18 (m, 4H; isopropyl CH), 1.48 ppm (d, ^3J(H,H) = 6.5 Hz, 24H; isopropyl CH_3); ^{13}C NMR (125 MHz, $CDCl_3$, 25 °C, TMS): $\delta = 24.92$, 35.66, 120.66, 126.69, 129.12, 132.01, 132.24, 134.40, 142.05, 145.55, 150.46, 151.95, 174.13 ppm; IR: $\tilde{\nu} = 3300$–2800 (broad), 3119, 3033, 2809, 1698, 1544, 1440, 1396, 1367, 1290, 1119, 1054, 990, 790, 759, 693 cm^{-1}; UV/Vis (CH_2Cl_2): λ_{max} (log ε) = 457 (5.91), 590 (4.96), 634 nm (4.76); MS (MALDI-TOF): *m/z* calcd for $C_{68}H_{56}N_4O_8Zn$: 1120.339; found: 1120.366.

5c: Greenish-brown solid (75%); m.p. > 330 °C; ^{1}H NMR (500 MHz, $CDCl_3$, 25 °C, TMS): $\delta = 8.59$ (s, 4H; β-H), 7.95 (d, ^3J(H,H) = 7.5 Hz, 8H; *o*-Ph-H), 7.74 (d, ^3J(H,H) = 8.0 Hz, 8H; *m*-Ph-H), 7.52 (s, 4H; fused-benzene-H), 1.60 ppm (s, 36H; *tert*-butyl-H); IR: $\tilde{\nu} = 3001$, 2962, 2919, 2850, 1712, 1419, 1358, 1259, 1219, 1091, 1009, 901, 791, 701 cm^{-1}; UV/Vis (CH_2Cl_2): λ_{max} (log ε) = 458 (6.04), 590 (5.39), 562 nm (5.35); MS (MALDI-TOF): *m/z* calcd for $C_{72}H_{64}N_4O_8Zn$: 1178.681; found: 1179.1.

5d: Greenish solid (70%); m.p. > 330 °C; ^{1}H NMR (500 MHz, $CDCl_3$, 25 °C, TMS): $\delta = 8.59$ (S, 4H; β-H), 7.94 (d, ^3J(H,H) = 6.5 Hz, 8H; *o*-Ph-H), 7.90 (s, 4H; fused-benzene-H), 7.27 (d, ^3J(H,H) = 6.5 Hz, 8H; *m*-Ph-H), 4.05 ppm (s, 12H; OCH_3); IR: $\tilde{\nu} = 3001$, 2962, 2919, 2850, 1712, 1419, 1358, 1259, 1219, 1091, 1009, 901, 791, 701 cm^{-1}; UV/Vis (CH_2Cl_2): λ_{max} (log ε) = 459 (6.05), 590 (5.38), 626 nm (5.30); MS (MALDI-TOF): *m/z* calcd for $C_{60}H_{40}N_4O_{12}Zn$: 1074.359; found: 1075.075.

5e: Greenish solid (60%); m.p. > 330 °C; ^{1}H NMR (500 MHz, $CDCl_3$, 25 °C, TMS): $\delta = 8.72$ (s, 4H; β-H), 8.47 (d, ^3J(H,H) = 15.5 Hz, 4H; alkenyl protons), 7.93 (d, ^3J(H,H) = 7.5 Hz, 8H; *o*-Ph-H), 7.65 (d, ^3J(H,H) = 7.5 Hz, 8H; *m*-Ph-H), 7.39 (s, 4H; fused-benzene-H), 6.09 (d, ^3J(H,H) = 15.5 Hz, 4H; alkenyl protons), 2.76 ppm (s, 12H; CH_3); UV/Vis (CH_2Cl_2): λ_{max} (log ε) = 471 (5.95), 596 (5.13), 638 (4.86); MS (MALDI-TOF): *m/z* calcd for $C_{68}H_{48}N_4O_8Zn$: 1114.510; found: 1115.018.

Acknowledgements

H.W. thanks Miami University and the Ohio Board of Reagents (Research Incentive Grant) for financial support. C.S.H. acknowledges support from the U.S Air Force Office of Scientific Research (Award no. FA9550-10-1-0377). The National Science Foundation (CHE0839233) is acknowledged for providing funds to purchase the MALDI TOF mass spectrometer that was used in this work.

---

[1] a) R. A. J. Thomas W. Hamann, A. B. F. Martinson, H. Van Ryswyk, J. T. Hupp, *Energy Environ. Sci.* **2008**, *1*, 66–78; b) N. Robertson, *Photonics Spectra* **2008**, *42*, 48; c) N. Robertson, *Angew. Chem.* **2008**, *120*, 1028–1030; *Angew. Chem. Int. Ed.* **2008**, *47*, 1012–1014; d) N. Robertson, *Angew. Chem.* **2006**, *118*, 2398–2405; *Angew. Chem. Int. Ed.* **2006**, *45*, 2338–2345; e) B. O'Regan, M. Grätzel, *Nature* **1991**, *353*, 737–740; f) A. B. F. Martinson, T. W. Hamann, M. J. Pellin, J. T. Hupp, *Chem. Eur. J.* **2008**, *14*, 4458–4467.

[2] a) Y. Xie, P. Joshi, M. Ropp, D. Galipeau, L. F. Zhang, H. Fong, Y. J. You, Q. Q. Qiao, *J. Porphyrins Phthalocyanines* **2009**, *13*, 903–909; b) S. Ito, S. M. Zakeeruddin, R. Humphry-Baker, P. Liska, R. Charvet, P. Comte, M. K. Nazeeruddin, P. Pechy, M. Takata, H. Miura, S. Uchida, M. Grätzel, *Adv. Mater.* **2006**, *18*, 1202; c) W. M. Campbell, A. K. Burrell, D. L. Officer, K. W. Jolley, *Coord. Chem. Rev.* **2004**, *248*, 1363–1379; d) L. Schmidt-Mende, U. Bach, R. Humphry-Baker, T. Horiuchi, H. Miura, S. Ito, S. Uchida, M. Grätzel, *Adv. Mater.* **2005**, *17*, 813; e) L. Schmidt-Mende, W. M. Campbell, Q. Wang, K. W. Jolley, D. L. Officer, M. K. Nazeeruddin, M. Grätzel, *ChemPhysChem* **2005**, *6*, 1253–1258; f) J. R. Durrant, S. A. Haque, E. Palomares, *Chem. Commun.* **2006**, 3279–3289; g) J. Rochford, D. Chu, A. Hagfeldt, E. Galoppini, *J. Am. Chem. Soc.* **2007**, *129*, 4655–4665; h) J. T. Dy, K. Tamaki, Y. Sanehira, J. Nakazaki, S. Uchida, T.

Kubo, H. Segawa, *Electrochemistry* **2009**, *77*, 206–209; i) H. Imahori, S. Hayashi, H. Hayashi, A. Oguro, S. Eu, T. Umeyama, Y. Matano, *J. Phys. Chem. C* **2009**, *113*, 18406–18413; j) A. J. Mozer, M. J. Griffith, G. Tsekouras, P. Wagner, G. G. Wallace, S. Mori, K. Sunahara, M. Miyashita, J. C. Earles, K. C. Gordon, L. C. Du, R. Katoh, A. Furube, D. L. Officer, *J. Am. Chem. Soc.* **2009**, *131*, 15621; k) M. Linke-Schaetzel, C. E. Anson, A. K. Powell, G. Buth, E. Palomares, J. D. Durrant, T. S. Balaban, J. M. Lehn, *Chem. Eur. J.* **2006**, *12*, 1931–1940.

[3] M. K. Nazeeruddin, R. Humphry-Baker, D. L. Officer, W. M. Campbell, A. K. Burrell, M. Grätzel, *Langmuir* **2004**, *20*, 6514–6517.

[4] a) W. M. Campbell, K. W. Jolley, P. Wagner, K. Wagner, P. J. Walsh, K. C. Gordon, L. Schmidt-Mende, M. K. Nazeeruddin, Q. Wang, M. Grätzel, D. L. Officer, *J. Phys. Chem. C* **2007**, *111*, 11760–11762; b) Q. Wang, W. M. Carnpbell, E. E. Bonfantani, K. W. Jolley, D. L. Officer, P. J. Walsh, K. Gordon, R. Humphry-Baker, M. K. Nazeeruddin, M. Grätzel, *J. Phys. Chem. B* **2005**, *109*, 15397–15409.

[5] a) C. W. Lee, H. P. Lu, C. M. Lan, Y. L. Huang, Y. R. Liang, W. N. Yen, Y. C. Liu, Y. S. Lin, E. W. G. Diau, C. Y. Yeh, *Chem. Eur. J.* **2009**, *15*, 1403–1412; b) C. F. Lo, S. J. Hsu, C. L. Wang, Y. H. Cheng, H. P. Lu, E. W. G. Diau, C. Y. Lin, *J. Phys. Chem. C* **2010**, *114*, 12018–12023; c) C. Y. Lin, C. F. Lo, L. Luo, H. P. Lu, C. S. Hung, E. W. G. Diau, *J. Phys. Chem. C* **2009**, *113*, 755–764; d) H. P. Lu, C. L. Mai, C. Y. Tsia, S. J. Hsu, C. P. Hsieh, C. L. Chiu, C. Y. Yeh, E. W. G. Diau, *Phys. Chem. Chem. Phys.* **2009**, *11*, 10270–10274; e) C. Y. Lee, C. X. She, N. C. Jeong, J. T. Hupp, *Chem. Commun.* **2010**, *46*, 6090–6092; f) C. P. Hsieh, H. P. Lu, C. L. Chiu, C. W. Lee, S. H. Chuang, C. L. Mai, W. N. Yen, S. J. Hsu, E. W. G. Diau, C. Y. Yeh, *J. Mater. Chem.* **2010**, *20*, 1127–1134; g) C. L. Wang, Y. C. Chang, C. M. Lan, C. F. Lo, E. W. G. Diau, C. Y. Lin, *Energy Environ. Sci.* **2011**, *4*, 1788–1795; h) Y. C. Chang, C. L. Wang, T. Y. Pan, S. H. Hong, C. M. Lan, H. H. Kuo, C. F. Lo, H. Y. Hsu, C. Y. Lin, E. W. G. Diau, *Chem. Commun.* **2011**, *47*, 8910–8912; i) T. Bessho, S. M. Zakeeruddin, C. Y. Yeh, E. W. G. Diau, M. Grätzel, *Angew. Chem.* **2010**, *122*, 6796–6799; *Angew. Chem. Int. Ed.* **2010**, *49*, 6646–6649; j) S. L. Wu, H. P. Lu, H. T. Yu, S. H. Chuang, C. L. Chiu, C. W. Lee, E. W. G. Diau, C. Y. Yeh, *Energy Environ. Sci.* **2010**, *3*, 949–955; k) A. Yella, H. W. Lee, H. N. Tsao, C. Y. Yi, A. K. Chandiran, M. K. Nazeeruddin, E. W. G. Diau, C. Y. Yeh, S. M. Zakeeruddin, M. Grätzel, *Science* **2011**, *334*, 629–634.

[6] a) M. S. Kang, J. B. Oh, K. D. Seo, H. K. Kim, J. Park, K. Kim, N. G. Park, *J. Porphyrins Phthalocyanines* **2009**, *13*, 798–804; b) S. Hayashi, Y. Matsubara, S. Eu, H. Hayashi, T. Umeyama, Y. Matano, H. Imahori, *Chem. Lett.* **2008**, *37*, 846–847; c) S. Hayashi, M. Tanaka, H. Hayashi, S. Eu, T. Umeyama, Y. Matano, Y. Araki, H. Imahori, *J. Phys. Chem. C* **2008**, *112*, 15576–15585.

[7] H. Imahori, T. Umeyama, S. Ito, *Acc. Chem. Res.* **2009**, *42*, 1809–1818.

[8] a) S. Eu, S. Hayashi, T. Urneyama, Y. Matano, Y. Araki, H. Imahori, *J. Phys. Chem. C* **2008**, *112*, 4396–4405; b) A. Kira, Y. Matsubara, H. Iijima, T. Umeyama, Y. Matano, S. Ito, M. Niemi, N. V. Tkachenko, H. Lemmetyinen, H. Imahori, *J. Phys. Chem. C* **2010**, *114*, 11293–11304; c) S. Mathew, H. Iijima, Y. Toude, T. Umeyama, Y. Matano, S. Ito, N. V. Tkachenko, H. Lemmetyinen, H. Imahori, *J. Phys. Chem. C* **2011**, *115*, 14415–14424; d) H. Imahori, H. Iijima, H. Hayashi, Y. Toude, T. Umeyama, Y. Matano, S. Ito, *ChemSusChem* **2011**, *4*, 797–805.

[9] a) O. Finikova, A. Cheprakov, I. Beletskaya, S. Vinogradov, *Chem. Commun.* **2001**, 261–262; b) O. S. Finikova, S. E. Aleshchenkov, R. P. Brinas, A. V. Cheprakov, P. J. Carroll, S. A. Vinogradov, *J. Org. Chem.* **2005**, *70*, 4617–4628; c) O. S. Finikova, A. V. Cheprakov, S. A. Vinogradov, *J. Org. Chem.* **2005**, *70*, 9562–9572; d) K. Kurotobi, K. S. Kim, S. B. Noh, D. Kim, A. Osuka, *Angew. Chem.* **2006**, *118*, 4048–4051; *Angew. Chem. Int. Ed.* **2006**, *45*, 3944–3947; e) S. Baluschev, V. Yakutkin, T. Miteva, Y. Avlasevich, S. Chernov, S. Aleshchenkov, G. Nelles, A. Cheprakov, A. Yasuda, K. Mullen, G. Wegner, *Angew. Chem.* **2007**, *119*, 7837–7840; *Angew. Chem. Int. Ed.* **2007**, *46*, 7693–7696; f) C. Borek, K. Hanson, P. I. Djurovich, M. E. Thompson, K. Aznavour, R. Bau, Y. R. Sun, S. R. Forrest, J. Brooks, L. Michalski, J. Brown, *Angew. Chem.* **2007**, *119*, 1127–1130; *Angew. Chem. Int. Ed.* **2007**, *46*, 1109–1112; g) Y. Sun, C. Borek, K. Hanson, P. I. Djurovich, M. E. Thompson, J. Brooks, J. J. Brown, S. R. Forrest, *Appl. Phys. Lett.* **2007**, *90*, 213503; h) H. Yamada, D. Kuzuhara, T. Takahashi, Y. Shirnizu, K. Uota, T. Okujima, H. Uno, N. Ono, *Org. Lett.* **2008**, *10*, 2947–2950.

[10] a) S. Ito, T. Murashima, H. Uno, N. Ono, *Chem. Commun.* **1998**, 1661–1662; b) O. Ongayi, V. Gottumukkala, F. R. Fronczek, M. G. H. Vicente, *Bioorg. Med. Chem. Lett.* **2005**, *15*, 1665–1668; c) L. J. Jiao, E. H. Hao, F. R. Fronczek, M. G. H. Vicente, K. M. Smith, *Chem. Commun.* **2006**, 3900–3902; d) M. G. H. Vicente, L. Jaquinod, R. G. Khoury, A. Y. Madrona, K. M. Smith, *Tetrahedron Lett.* **1999**, *40*, 8763–8766; e) M. G. H. Vicente, A. C. Tome, A. Walter, J. A. S. Cavaleiro, *Tetrahedron Lett.* **1997**, *38*, 3639–3642; f) W. Liu, F. R. Fronczek, M. G. H. Vicente, K. M. Smith, *Tetrahedron Lett.* **2005**, *46*, 7321–7324; g) M. A. Filatov, A. Y. Lebedev, S. A. Vinogradov, A. V. Cheprakov, *J. Org. Chem.* **2008**, *73*, 4175–4185; h) O. S. Finikova, A. V. Cheprakov, I. P. Beletskaya, P. J. Carroll, S. A. Vinogradov, *J. Org. Chem.* **2004**, *69*, 522–535; i) O. S. Finikova, A. V. Cheprakov, P. J. Carroll, S. A. Vinogradov, *J. Org. Chem.* **2003**, *68*, 7517–7520; j) A. M. G. Silva, K. T. de Oliveira, M. A. F. Faustino, M. Neves, A. C. Tome, A. M. S. Silva, J. A. S. Cavaleiro, P. Brandao, V. Felix, *Eur. J. Org. Chem.* **2008**, 704–712; k) A. Pereira, C. M. A. Alonso, M. Neves, A. C. Tome, A. M. S. Silva, F. A. A. Paz, J. A. S. Cavaleiro, *J. Org. Chem.* **2008**, *73*, 7353–7356; l) A. C. Tomé, P. S. S. Lacerda, M. Neves, J. A. S. Cavaleiro, *Chem. Commun.* **1997**, 1199–1200.

[11] R. Deshpande, L. Jiang, G. Schmidt, J. Rakovan, X. P. Wang, K. Wheeler, H. Wang, *Org. Lett.* **2009**, *11*, 4251–4253.

[12] a) H. L. Anderson, *Chem. Commun.* **1999**, 2323–2330; b) A. Ceulemans, W. Oldenhof, C. Gorllerwalrand, L. G. Vanquickenborne, *J. Am. Chem. Soc.* **1986**, *108*, 1155–1163.

[13] U. Varetto, Molekel 5.4.0.8; Swiss National Supercomputing Centre, Manno, Switzerland.

[14] M. K. Nazeeruddin, A. Kay, I. Rodicio, R. Humphry-Baker, E. Müller, P. Liska, N. Vlachopoulos, M. Grätzel, *J. Am. Chem. Soc.* **1993**, *115*, 6382-6390.

[15] P. Rothemund, *J. Am. Chem. Soc.* **1936**, *58*, 625-627..

Received: June 7, 2012

***opp*-ortunity knocks**: Symmetrical *opp*-dibenzoporphyrins with various linkers and substituents were used as sensitizers for dye-sensitized solar cells. These porphyrins displayed moderate efficiency for the conversion of solar energy into electricity.

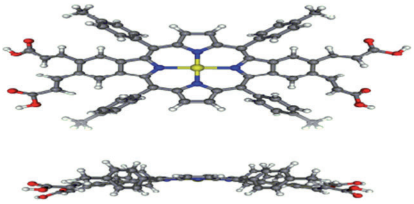

Dye-Sensitized Solar Cells

Rohit Deshpande, Bo Wang, Lin Dai,
Lin Jiang, C. Scott Hartley,
*Shouzhong Zou, Hong Wang,**
*Lei Kerr** ▮▮▮▮–▮▮▮▮

***Opp*-Dibenzoporphyrins as a Light-Harvester for Dye-Sensitized Solar Cells**
